European Journal of Radiology 110 (2019) 97–104

Contents lists available at ScienceDirect

European Journal of Radiology

journal homepage: www.elsevier.com/locate/ejrad

Research article

Virtual touch tissue imaging and quantification (VTIQ) in the evaluation of breast lesions: The associated factors leading to misdiagnosis

Jia-Wei Sun[1], Xiao-Lei Wang[1], Qing Zhao, Hang Zhou, Lin Tao, Zhao-Peng Jiang, Wan-Yu Zhang, Xian-Li Zhou*

In-Patient Ultrasound Department, Second Affiliated Hospital of Harbin Medical University, Harbin, China

ARTICLE INFO

Keywords:
Virtual touch tissue imaging and quantification
Breast lesion
Shear wave speed
False-positive
False-negative

ABSTRACT

Purpose: To investigate the factors that could cause a misdiagnosis in virtual touch tissue imaging and quantification (VTIQ) when differentiating benign and malignant breast lesions, and to analyze the imaging characteristics of those lesions with incorrect findings.

Methods: The conventional ultrasound (CUS) features and the VTIQ parameters of 153 benign lesions and 99 malignant lesions were retrospectively analyzed and compared with histopathological and/or core-needle biopsy (CNB)-proven results. Independent variables that led to inaccurate VTIQ results were selected by binary logistic regression analysis.

Results: The maximum shear wave speed (SWS-max), the mean SWS (SWS-mean), the minimum SWS (SWS-min), the lesion-to-fat SWS ratio (SWS-L/F), and the lesion-to-gland SWS ratio (SWS-L/G) in malignant lesions were significantly higher than those in benign lesions (all $P < 0.001$). The false-positive rate (FPR) of benign lesions and the false-negative rate (FNR) of malignant lesions were 9.8% and 19.2%, respectively, using an SWS-max cut-off value of 4.46 m/s. Diameter, depth, and posterior acoustic features were independent variables related to false-positive VTIQ findings (*P*: 0.049, 0.010 and 0.032, respectively). The invasive status and the histologic grade of infiltrating carcinoma were significantly associated with false-negative VTIQ findings (*P*: 0.026 and 0.015).

Conclusion: Diameter, depth, posterior acoustic features, invasive status, and histologic grade have a significant influence on the accuracy of VTIQ results, and these characteristics of breast lesions should be taken into account when interpreting the results of VTIQ examinations.

1. Introduction

The occurrence of breast cancer has been increasing recently in both developed and developing countries [1]. Conventional ultrasonography (CUS) is widely used in screening and evaluating breast lesions, and it is a convenient, cost-effective, and widely available method. However, it provides only morphological features of the breast lesion and is dependent on the operator's experience. Ultrasound elastography (USE) can evaluate the stiffness of the targeting tissue [2–4], and achieve promising results for the differentiation of malignant breast lesions from benign lesions [5–11]. USE includes strain elastography (SE) and shear wave elastography (SWE). SE measures the lesion stiffness with a qualitative assessment (i.e., "colour scale") and/or a semi-quantitative assessment (i.e., "strain ratio"). Compared to SE, the SWE technique can quantitatively reflect the mechanical properties of the lesion by measuring shear wave speed (SWS).

Recently, a two-dimensional (2D) SWE, Virtual Touch Imaging Quantification (VTIQ, Siemens Medical Solutions, Mountain View, CA,

Abbreviations: VTIQ, virtual touch tissue imaging and quantification; CUS, conventional ultrasound; CNB, core-needle biopsy; SWS, shear wave speed; SWS-L/F, lesion-to-fat SWS ratio; SWS-L/G, lesion-to-gland SWS ratio; FNR, false-negative rate; FPR, false-positive rate; IDC, infiltrating ductal carcinoma; DCIS, ductal carcinoma in situ; USE, ultrasound elastography; SE, strain elastography; SWE, shear wave elastography; 2D, two-dimensional; ROI, region of interest; ER, estrogen receptor; PR, progesterone receptor; HER2, human epidermal receptor type 2; QM, quality measurement; SD, standard deviation; ROC, receiver operating characteristic; Az, the area under the ROC curve; B, regression coefficient; OR, odds ratio; CI, confidence interval

* Corresponding author at: In-Patient Ultrasound Department, Second Affiliated Hospital of Harbin Medical University, Surgeons' Hall, No. 246. Xuefu Road, Nangang District, Harbin City, Heilongjiang Prov, China.
E-mail address: hrbzhouxl@163.com (X.-L. Zhou).
[1] These authors contributed equally to this work.

https://doi.org/10.1016/j.ejrad.2018.11.021
Received 1 September 2018; Received in revised form 15 November 2018; Accepted 19 November 2018

USA) has been introduced to evaluate breast lesions. This technique demonstrates a higher diagnostic performance for breast lesions than CUS [12,13]. Unfortunately, it should be noted that VTIQ led to wide ranges of false-negative rates (FNR: 11.9%–32.1%) and false-positive rates (FPR: 7.3%–20.2%) when a single SWS cut-off value was applied [9,11,12,14,15]. This indicates the need to explore the factors that are associated with these false-positive and false-negative VTIQ findings in clinical practice. Several reports have discussed the related factors that led to false SWE (Supersonic Imagine, Aix en Provence, France) findings of breast lesions [16–18]. But, to our knowledge, there are no reports in the literature about the factors that may lead to misdiagnosis using VTIQ for the assessment of breast lesions.

Therefore, we aim to investigate the factors associated with these false-positive and false-negative findings when using VTIQ to evaluate breast lesions.

2. Materials and methods

This retrospective study was approved by the institutional ethics committee, and informed consent was waived due to the retrospective nature of this study.

2.1. Patients

From April 2017 to July 2018, 430 cases of consecutive female patients with 450 solid breast lesions were retrospectively reviewed. According to the management recommendations of the ACR BI-RADS [19], breast lesions classified as category 4a, 4b, 4c, or 5 were recommended for tissue diagnosis by biopsy or surgery. BI-RADS 3 lesions were biopsied or surgically removed because of patients' requests or suspicious criteria assessed by other examinations, such as magnetic resonance imaging and mammography. The inclusion criteria were: (i) Breast lesions were referred to CUS and VTIQ according to standard protocols; (ii) patients with breast lesions underwent core-needle biopsy (CNB) and/or surgery and the breast lesions were confirmed by histopathological examinations; (iii) benign breast lesions on CNB were followed for at least 12 months; (iv) the largest diameter of breast lesions was smaller than the footprint of the transducer (40 mm); and (v) no invasive procedures, including endocrinotherapy, chemotherapy, or radiotherapy, were performed previously. There were 244 patients with 260 breast lesions who met the inclusion criteria and were enrolled in the study. Among them, seven patients with eight breast lesions were excluded since there was not enough fat tissue around the lesions to measure lesion-to-fat SWS ratio (SWS-L/F). For the patients with multiple breast lesions on one side of the breast, the most suspicious lesion according to the BI-RADS category was selected. For the patients with the same BI-RADS category on one side of the breast, the largest lesion was included. Finally, 252 breast lesions (mean diameter, 20.1 mm ± 8.0; range, 5.1 mm–39.1 mm) in 237 patients (mean age, 43.2 years ± 14.1; range, 18–77 years) were analyzed. A single lesion was detected in 222 patients and two lesions in 15 patients. All malignant breast lesions and 123 benign breast lesions were surgically removed. Thirty benign lesions with histopathological results on CNB were followed for at least 12 months without a change in size or CUS appearance. The following pathological features were recorded: pathological type; histologic type; histological grade for infiltrating carcinoma; invasive status; and axillary lymph node stage. Immunohistochemistry parameters, such as estrogen receptor (ER), progesterone receptor (PR), human epidermal receptor type 2 (HER2) status, and Ki-67 index, were recorded as well. The flowchart for patient selection is shown in Fig. 1.

2.2. CUS and VTIQ examinations

CUS and VTIQ examinations were both performed on Siemens S3000 equipment (Siemens Medical Solutions, Mountain View, CA, USA), equipped with a 9L4 linear array transducer (frequency range, 4–9 MHz). All lesions were examined by the same operator, who had 10 years of experience in breast CUS and was trained for three months to perform VTIQ examinations to guarantee optimized image quality before the study. CUS, including gray scale images and color Doppler bilateral breast images were performed with optimized machine settings, sufficient gel application, and with patients in the supine position. The target lesion was placed in the center of the screen. Gray scale images and color Doppler images of each target lesion were acquired on both transverse and longitudinal cross-sections. The largest area in the lesion was chosen for the longitudinal cross-section and the transverse cross-section was orthogonal to the longitudinal cross-section.

Subsequently, VTIQ was performed on the longitudinal cross-section of the lesion. During VTIQ image acquisition, the location of the transducer was immobile and perpendicular to the surface of the breast. The scanning pressure applied on the skin was as low as possible to reduce any artificial influence on the stiffness of the target lesion, and patients were asked to hold their breath for 3–5 s. VTIQ provides four imaging modes: (i) shear wave quality mode includes a 2D color map used to assess the quality measurement (QM) of SWS imaging, which shows colors from high (green) to intermediate (yellow) to low quality (red); (ii) shear wave velocity mode displays colors from high SWS (red) to intermediate SWS (yellow or green) to low SWS (blue); (iii) shear wave travel time mode; and (iv) shear wave displacement mode. The fixed diameter of the ROI box used to measure SWS was 2 mm. Each lesion, adjacent gland, and the fat tissue were measured seven times, respectively. The following points were noted when placing an ROI box in the lesion: (i) the area of the lesion coded by the highest and lowest SWS was selected, and the remaining measurements were randomly selected; (ii) to obtain the most optimal and reproducible SWS measurements, the operator selected the green areas from the shear wave quality mode in which to place the ROI; (iii) areas with liquid or calcification were not allowed to be selected. Usually, a radiologist spent about 5–10 min on the whole procedure. All the images were stored for further analysis.

2.3. Image interpretation and analysis

CUS images were independently reviewed by two other radiologists who had at least five years of experience in breast CUS and four years of experience in breast USE. They were blinded to the pathological results. Differing opinions were resolved through consensus.

The following CUS features of the breast lesions were evaluated: size (the largest diameter); position (upper outer quadrant, upper inner quadrant, lower outer quadrant, lower inner quadrant); depth (distance from the skin to the superficial surface of the lesion); distance from the nipple (distance from the medial margin of the lesion to the center of nipple); shape (oval, round, irregular); orientation (parallel, not parallel); margin (circumscribed, non-circumscribed); echo pattern (hyperechoic, isoechoic, hypoechoic, heterogeneous); posterior acoustic features (shadowing, no posterior acoustic features, enhancement, combined pattern); internal calcifications feature (present, absent); and vascularity (absent vessels, vessels in rim, rare internal vessels with or without peripheral vessels, internal vascularity with or without peripheral vessels). The depth was divided into three groups: ≤ 3 mm; > 3 mm and ≤ 7 mm; and > 7 mm. The distance from the nipple was divided into two groups: ≤ 20 mm; and > 20 mm. In our research, the combined pattern of posterior acoustic features was the combination of enhancement and shadowing. Thus, the shadowing and combined pattern were all characterized as shadowing. Meanwhile, the lesions were classified according to the ACR BI-RADS categories [19].

In the VTIQ mode, the maximum SWS of the lesion (SWS-max), the minimum SWS of the lesion (SWS-min), the mean SWS of the lesion (SWS-mean), the SWS-L/F, and the lesion-to-gland SWS ratio (SWS-L/G) were obtained and calculated for analysis. In the shear wave quality mode of the VTIQ, the level of QM was evaluated as low or high [20]. If the lesion and surrounding rim appeared yellow or red in color, the QM of the lesion was regarded as low. However, if the whole lesion was covered by the green color, the QM of the lesion was regarded as high.

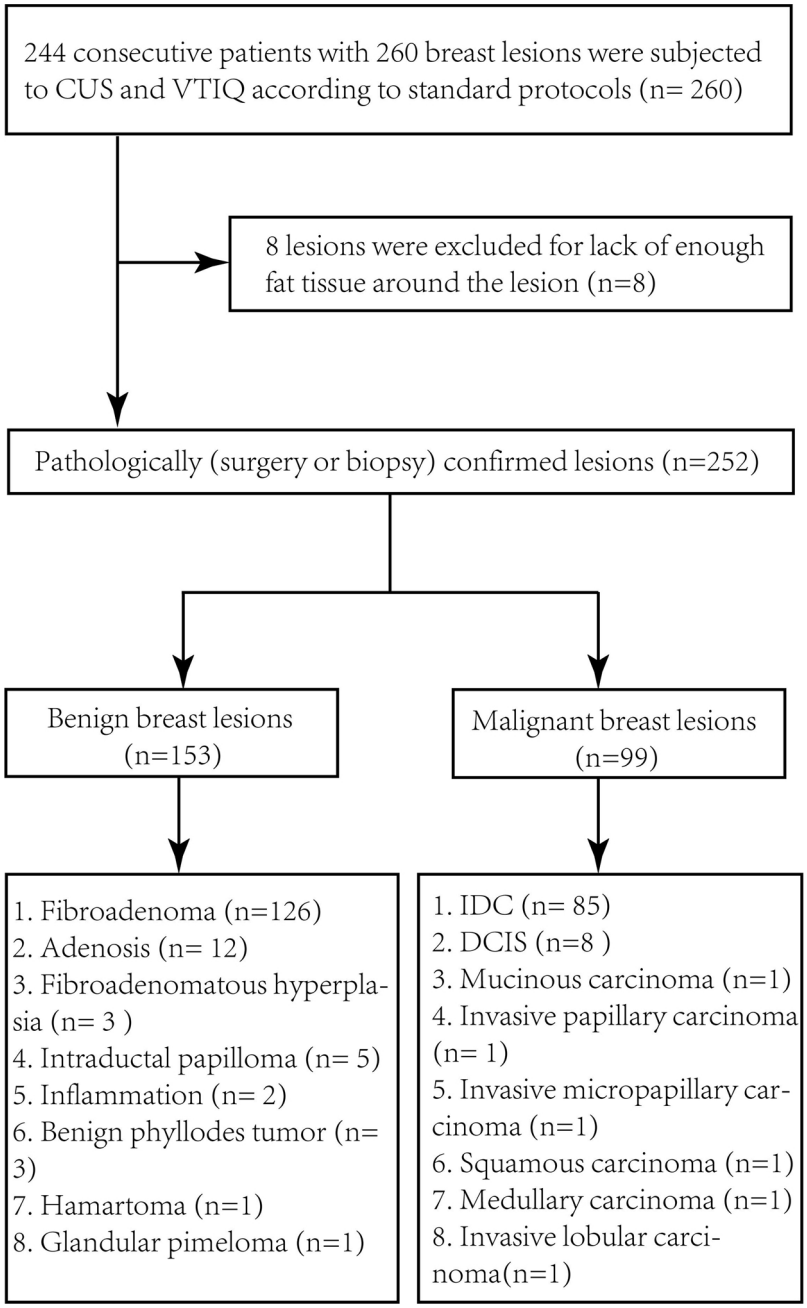

Fig. 1. Flowchart of breast lesion selection. IDC = infiltrating ductal carcinoma; DCIS = ductal carcinoma in situ.

The VTIQ features were compared with the final histopathology results and were further divided into 'true' and 'false' groups among the benign and malignant lesions as follows. Benign lesions that had an SWS value less than that of the best cut-off value were classified as 'true negative;' however, pathologically proven benign lesions that had an SWS value greater than that of the best cut-off value were classified as 'false positive.' Pathologically proven malignant lesions that had an SWS value less than that of the best cut-off value were classified as 'false negative,' and pathologically proven malignant lesions that had an SWS value greater than that of the best cut-off value were classified as 'true positive.'

2.4. Statistical analysis

Statistical analyses of the current study were calculated using SPSS version 20.0 (IBM corporation, Armonk, NY, USA) software. The continuous quantitative data were expressed as the mean ± standard deviation (SD). The continuous quantitative data with a normal distribution were analyzed using an independent *t*-test The remaining continuous quantitative data with a skewed distribution were analyzed using a Mann-Whitney U test. The Chi-square test or Fisher's exact test was applied for categorical variables. The receiver operating characteristic (ROC) curve was used to evaluate the diagnostic performances of SWS values (including SWS-max, SWS-mean, SWS-min, SWS-L/F, and SWS-L/G). The optimal cut-off values were obtained when the Youden index (sensitivity + specificity - 1) was maximum. The area under the ROC curve (Az) was obtained for each SWS parameter. We used the SWS parameter with the highest Az value in this study. Binary logistic regression analysis with an "Enter" selection method was performed to select independent variables. The independent variables with *P* values less than 0.05 in the multivariate logistic regression analysis were selected for odds ratios (ORs), with the calculation of 95% confidence intervals (CIs). All tests were two-sided, and *P* values less than

Table 1
SWS measurement results and the QM on shear wave quality images in benign and malignant breast lesions.

Parameters	Benign	Malignant	*p* value
SWS-mean (m/s)[a]	2.75 ± 0.75 (1.14–5.95)	5.18 ± 1.68 (1.78–9.15)	< 0.001*
SWS-max (m/s)[a]	3.23 ± 1.13 (1.28–9.50)	6.76 ± 2.20 (2.05–9.99)	< 0.001*
SWS-min (m/s)[a]	2.30 ± 0.60 (0.94–4.41)	3.87 ± 1.43 (1.52–7.97)	< 0.001*
SWS-L/F[a]	1.70 ± 0.47 (0.69–3.53)	3.17 ± 1.29 (1.08–7.49)	< 0.001*
SWS-L/G[a]	1.44 ± 0.43 (0.67–2.90)	2.53 ± 1.06 (0.73–6.26)	< 0.001*
QM			0.013*
Low QM[b](n = 40)	17 (11.1%)	23 (23.2%)	
High QM[b] (n = 212)	136 (88.9%)	76 (76.8%)	

[a] Data are mean values ± standard deviations, and the value ranges are in parentheses.
[b] Numbers in parentheses are percentage of benign and malignant lesions. SWS = shear wave speed, SWS-L/F = lesion-to-fat SWS ratio, SWS-L/G = lesion-to-gland SWS ratio, QM = quality measurement.
* Indicates statistically significant difference.

0.05 were considered statistically significant.

3. Results

There were 99 (39.3%) malignant breast lesions and 153 (60.7%) benign breast lesions. The pathological results of the breast lesions are shown in Fig. 1.

3.1. VTIQ parameters for the differentiation of benign and malignant breast lesions

All the quantitative VTIQ parameters in malignant breast lesions (including SWS-mean, SWS-max, SWS-min, SWS-L/F and SWS-L/G) were significantly higher than those in benign breast lesions (all $P <$ 0.001), and the level of QM was significantly different between benign breast lesions and malignant lesions ($P =$ 0.013) (Table 1).

Among the quantitative VTIQ parameters, SWS-max achieved the highest Az value. The optimal cut-off value of SWS-max was 4.46 m/s, with a sensitivity of 80.8% (80/99), a specificity of 90.2% (138/153), an accuracy of 86.5% (218/252), a PPV of 84.2% (80/95), and an NPV of 87.9% (138/157) (Table 2).

3.2. Influential factors for false VTIQ findings

When an SWS-max cut-off value of 4.46 m/s was applied, the FPR was 9.8% (15/153) and the FNR was 19.2% (19/99). The significant features for differentiation between true-negative breast lesions and false-positive lesions were diameter, depth, distance from the nipple, echo pattern, posterior acoustic features, and BI-RADS category (all $P <$ 0.05) (Table 3). For malignant breast lesions, internal calcifications, BI-RADS category, histologic grade of infiltrating carcinomas, and invasive status were significant predictors for false-negative VTIQ when compared with true-positive VTIQ findings (all $P <$ 0.05) (Table 3). The pathological type of false-positive VTIQ results comprised fibroadenoma (n = 12; 9.5%, 12/126) (Fig. 2), inflammation (n = 1; 50%, 1/2), adenosis (n = 1; 8.3%, 1/12), and fibroadenomatous hyperplasia (n = 1; 33.3%, 1/3). The pathological type of false-negative VTIQ results comprised infiltrating ductal carcinoma (IDC) (n = 13; 15.3%, 13/85), ductal carcinoma in situ (DCIS) (n = 5; 62.5%, 5/8) (Fig. 3), and medullary carcinoma (n = 1; 100%, 1/1). For infiltrating carcinomas, the histologic grade was significantly different between true-positive VTIQ findings and false-negative VTIQ findings (Table 3). Immunohistochemistry status (including ER, PR, HER-2, and Ki-67 index) was not associated with false-negative VTIQ findings (Table 3).

3.3. Multivariate logistic regression analysis

Binary logistic regression analysis showed that diameter, depth, and posterior acoustic features were independent characteristics associated with false-positive VTIQ results (*P*: 0.049, 0.010, 0.032, respectively) (Table 4). The larger lesions were more often seen with the false-positive VTIQ results. False-positive results were more likely to appear for breast lesions with a depth of ≤3 mm (Fig. 2) or on lesions that had the posterior acoustic features of shadowing and a combined pattern. For infiltrating carcinomas, lesions with a histologic grade of 1 were more likely to show false-negative VTIQ results than those with a grade 2 or 3 (*P*: 0.015) (Table 5). False-negative VTIQ findings were more likely to occur with non-invasive carcinomas (Fig. 3) than with invasive carcinomas (β: 1.832, OR: 6.193, 95% CI: 1.246–30.790, *P*: 0.026) (Table 6).

4. Discussion

In this study, VTIQ parameters in malignant breast lesions were significantly higher than those in benign lesions, including SWS-mean, SWS-max, SWS-min, SWS-L/F, and SWS-L/G. SWS-max had the highest Az value among all parameters, with 80.8% sensitivity, 90.2% specificity, 84.2% PPV, 87.9% NPV, and 86.5% accuracy, using a cut-off value of 4.46 m/s. The high level of QM was observed mostly in benign breast lesions, which is consistent with a previous study [20].

Although VTIQ is a highly accurate and reliable elastography method for the evaluation of breast lesions with regard to promising intra- and inter-examiner agreement [21], we still encounter VTIQ results that are contrary to the final histopathological diagnoses in the clinical routine. Unfortunately, there is little research that has

Table 2
Diagnostic performance of SWS measurement parameters.

Parameters	Cut-off value	Sensitivity (%)	Specificity (%)	Accuracy (%)	PPV (%)	NPV (%)	Az (95% CI)	*P* value
SWS-mean	3.80 m/s	78.8(78/99)	92.8(141/153)	86.9(219/252)	86.7(78/90)	87.0(141/162)	0.905(0.865-0.946)	< 0.001*
SWS-max	4.46 m/s	80.8(80/99)	90.2(138/153)	86.5(218/252)	84.2(80/95)	87.9(138/157)	0.913(0.874-0.951)	< 0.001*
SWS-min	2.90 m/s	75.8(75/99)	85.6(131/153)	81.7(206/252)	77.3(75/97)	84.5(131/155)	0.863(0.816-0.911)	< 0.001*
SWS-L/F	2.34	72.7(72/99)	92.2(141/153)	84.5(213/252)	85.7(72/84)	83.9(141/168)	0.873(0.825-0.920)	< 0.001*
SWS-L/G	2.01	64.6(64/99)	91.5(140/153)	81.0(204/252)	83.1(64/77)	80.0(140/175)	0.842(0.791-0.893)	< 0.001*

Data were tested with the area under the receiver operating characteristic (ROC) curve. SWS = shear wave speed, SWS-L/F = lesion-to-fat SWS ratio, SWS-L/G = lesion-to-gland SWS ratio. PPV = positive predictive value, NPV = negative predictive value, Az = the area under the ROC curve, CI = confidence interval.
* Indicates statistically significant difference.

Table 3
Analyzing the correlation of the characteristics of patients, CUS imaging, histopathology features and immunohistochemistry status of breast lesions with SWS-max findings by univariate analysis.

Characteristics	Benign breast lesions			Malignant breast lesions		
	SWS-max			SWS-max		
	< 4.46 m/s(n = 138)	≥ 4.46 m/s(n = 15)	P-value	< 4.46 m/s(n = 19)	≥ 4.46 m/s(n = 80)	P-value
Age (yrs)[#]	36.6 ± 11.5	33.9 ± 12.2	0.396	52.9 ± 9.5	54.0 ± 11.3	0.880
Diameter (mm)[#]	18.5 ± 7.8	28.9 ± 8.7	0.006*	19.0 ± 7.8	22.1 ± 7.9	0.119
Lesion position[b]			0.635			0.052
Upper outer quadrant	78 (51.0%)	9 (5.9%)		9 (9.1%)	44 (44.4%)	
Upper inner quadrant	19 (12.4%)	2 (1.3%)		6 (6.1%)	15 (15.2%)	
Lower outer quadrant	28 (18.3%)	4 (2.6%)		0 (0.0%)	15 (15.2%)	
Lower inner quadrant	13 (8.5%)	0 (0.0%)		4 (4.0%)	6 (6.1%)	
Depth (mm)[#,b]	6.2 ± 3.8	4.9 ± 2.8	0.012*	7.7 ± 3.3	6.1 ± 3.0	0.096
≤3	35 (22.9%)	9 (5.9%)	0.018*	3 (3.0%)	13 (13.1%)	0.074
> 3,≤7	61 (39.9%)	4 (2.6%)		5 (5.1%)	42 (42.4%)	
> 7	42 (27.4%)	2 (1.3%)		11 (11.1%)	25 (25.3%)	
Distance from the nipple (mm)[#,b]	22.6 ± 16.2	12.7 ± 13.6	0.019*	31.0 ± 21.4	28.1 ± 17.4	0.541
≤20	70 (45.8%)	12 (7.8%)	0.053	8 (8.1%)	28 (28.3%)	0.602
> 20	68 (44.4%)	3 (2.0%)		11 (11.1%)	52 (52.5%)	
Shape[b]			0.641			0.210
Oval	117 (76.5%)	11 (7.2%)		3 (3.0%)	4 (4.0%)	
Round	2 (1.3%)	0 (0.0%)		0 (0.0%)	2 (2.0%)	
Irregular	19 (12.4%)	4 (2.6%)		16 (16.2%)	74 (74.8%)	
Orientation[b]						0.282
Parallel	131 (85.6%)	14 (9.2%)		15 (15.2%)	50 (50.5%)	
Not parallel	7 (4.6%)	1 (0.6%)		4 (4.0%)	30 (30.3%)	
Margin[b]			0.187			0.580
Circumscribed	118 (77.1%)	12 (7.8%)		1 (1.0%)	3 (3.0%)	
Non-circumscribed	20 (13.1%)	3 (2.0%)		18 (18.2%)	77 (77.8%)	
Echo pattern[b]			0.006*			0.159
Hyperechoic	1 (0.6%)	0 (0.0%)		0 (0.0%)	0 (0.0%)	
Isoechoic	49 (32.0%)	4 (2.6%)		3 (3.0%)	5 (5.1%)	
Hypoechoic	76 (49.7%)	6 (3.9%)		14 (14.1%)	53 (53.5%)	
Heterogeneous	12 (7.8%)	5 (3.3%)		2 (2.0%)	22 (22.2%)	
Posterior acoustic features[b]			0.001*			0.106
Shadowing	5 (3.3%)	0 (0.0%)		4 (4.0%)	6 (6.1%)	
No posterior acoustic features	57 (37.2%)	4 (2.6%)		7 (7.1%)	32 (32.3%)	
Enhancement	71 (46.4%)	7 (4.6%)		7 (7.1%)	22 (22.2%)	
Combined pattern	5 (3.3%)	4 (2.6%)		1 (1.0%)	20 (20.2%)	
Internal calcifications[b]			1.000			0.042*
Present	17 (11.1%)	1 (0.6%)		6 (6.1%)	47 (47.5%)	
Absent	121 (79.1%)	14 (9.2%)		13 (13.1%)	33 (33.3%)	
Vascularity[b]			0.678			0.074
Absent vessels	34 (22.2%)	3 (2.0%)		2 (2.0%)	2 (2.0%)	
Vessels in rim	17 (11.1%)	2 (1.3%)		4 (4.0%)	8 (8.1%)	
Rare internal vessels	23 (15.0%)	1 (0.6%)		4 (4.0%)	9 (9.1%)	
Internal vascularity	64 (41.8%)	9 (5.9%)		9 (9.1%)	61 (61.6%)	
BI-RADS category[b]			0.016*			0.025*
3	114 (74.5%)	11 (7.2%)		1 (1.0%)	0 (0.0%)	
4a	23 (15.0%)	3 (2.0%)		3 (3.0%)	8 (8.1%)	
4b	6 (3.9%)	0 (0.0%)		6 (6.1%)	11 (11.1%)	
4c	0 (0.0%)	1 (0.6%)		7 (7.1%)	30 (30.3%)	
5	0 (0.0%)	0 (0.0%)		2 (2.0%)	31 (31.3%)	
Histologic type[b]						0.324
Ductal				17 (17.2%)	76 (76.8%)	
Other				2 (2.0%)	4 (4.0%)	
Axillary lymph node metastasis[b]						0.800
Positive				8 (8.1%)	38 (38.4%)	
Negative				11 (11.1%)	42 (42.4%)	
Histologic grade[a, b]						0.003*
Grade 1				4 (4.4%)	3 (3.3%)	
Grade 2				2 (2.2%)	30 (33.0%)	
Grade 3				8 (8.8%)	44 (48.3%)	
Invasive status[b]						0.006*
Invasive				14 (14.1%)	77 (77.8%)	
Non-invasive				5 (5.1%)	3 (3.0%)	
Immunohistochemistry status						
ER-positive[b]				13 (13.1%)	62 (62.6%)	0.390
ER-negative[b]				6 (6.1%)	18 (18.2%)	
PR–positive[b]				12 (12.1%)	62 (62.6%)	0.242
PR- negative[b]				7 (7.1%)	18 (18.2%)	
HER-2–positive[b]				13 (13.1%)	53 (53.5%)	1.000
HER-2– negative [b]				6 (6.1%)	27 (27.3%)	

(*continued on next page*)

Table 3 (*continued*)

Characteristics	Benign breast lesions			Malignant breast lesions		
	SWS-max			SWS-max		
	< 4.46 m/s(n = 138)	≥ 4.46 m/s(n = 15)	P-value	< 4.46 m/s(n = 19)	≥ 4.46 m/s(n = 80)	P-value
Ki-67 index (%)[#]				36.1 ± 30.7	40.0 ± 24.8	0.321

CUS = conventional ultrasound, SWS = shear wave speed, BI-RADS = breast imaging reporting and data system, ER = estrogen receptor, PR = progesterone receptor, HER2 = human epidermal growth factor receptor 2.

[a] Data are the histologic grade of invasive carcinomas (n = 91).

[b] Numbers in parentheses are percentage of benign and malignant lesions.

[#] Data are means ± standard deviations.

[*] Indicates statistically significant difference.

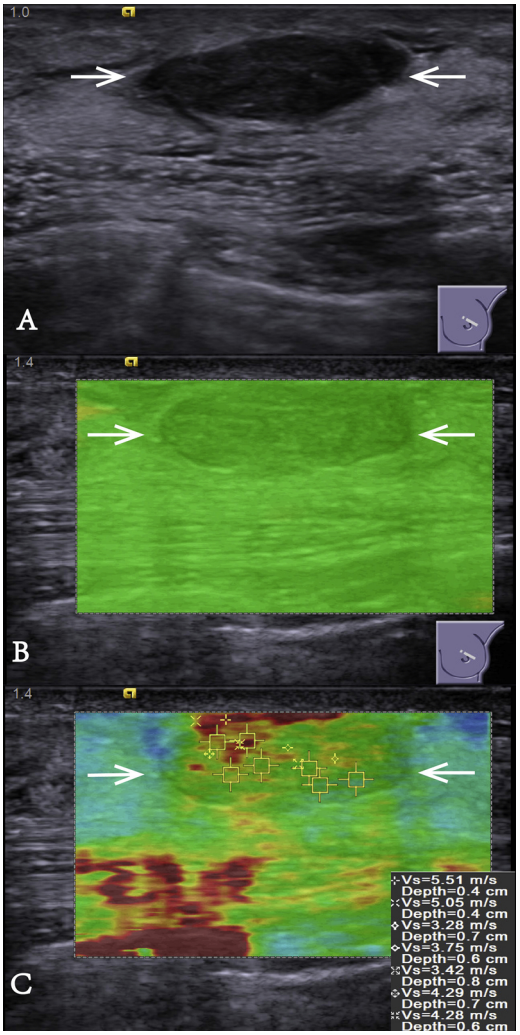

Fig. 2. False-positive VTIQ results in a 29-year-old woman. Histopathological results after surgery indicated that this breast lesion was a fibroadenoma. (A) Conventional ultrasound shows a 20.5 mm breast lesion classified as 3 on B-mode, which appears as oval-shaped, with a circumscribed margin, hypoechogenic, parallel, and with enhancement posterior acoustic. The distance from the skin to the superficial surface of the lesion was 2 mm. (B) Shear wave quality mode: the green color represents a high level QM of SWS imaging. (C) The SWS measurement of the breast lesion. SWS-max was 5.51 m/s. VTIQ = virtual touch tissue imaging and quantification, SWS = shear wave speed, QM = quality measurement.

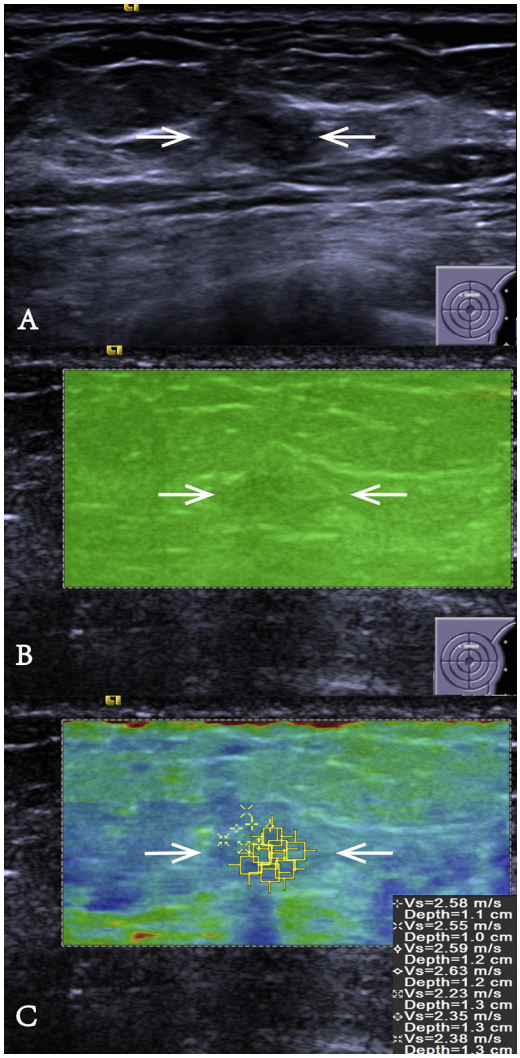

Fig. 3. False-negative VTIQ results in a 49-year-old woman. Histopathological results after surgery for this breast lesion indicated a DCIS with no axillary node metastasis. This lesion was assigned a histologic grade of 1. ER: positive, PR: negative, HER-2: positive, Ki-67: 25%. (A) Conventional ultrasound shows a 6.0 mm breast lesion classified as 4a on B-mode that appears oval-shaped, with a non-circumscribed margin, isoechoic, parallel, and with no posterior acoustic feature. The distance from the skin to the superficial surface of the lesion was 8 mm. (B) Shear wave quality mode: the green color represents a high level QM of SWS imaging. (C) The SWS measurement of the breast lesion. SWS-max was 2.63 m/s. VTIQ = virtual touch tissue imaging and quantification, DCIS = ductal carcinoma in situ, ER = estrogen receptor, PR = progesterone receptor, HER2 = human epidermal growth factor receptor 2, QM = quality measurement, SWS = shear wave speed.

investigated the factors that lead to a misdiagnosis using VTIQ to differentiate benign breast lesions from malignant lesions. When we applied a single SWS-max cut-off value to diagnose breast lesions, the FPR

Table 4
Independent factors related to false positive VTIQ finding of benign breast lesions.

Characteristics	β	OR	95% CI	*P* value
Diameter (mm)	0.107	1.112	1.001–1.237	0.049*
Depth				
> 7 (mm)				0.010*
> 3 (mm), ≤7 (mm)	−0.713	0.490	0.050–4.818	0.541
≤3 (mm)	2.689	14.714	1.492–145.158	0.021*
Distance from the nipple(mm)	−0.030	0.971	0.924–1.019	0.232
Echo pattern				
Heterogeneous				0.123
Hyperechoic	−17.478	0.000	0.000	1.000
Isoechoic	−2.063	0.127	0.019–0.848	0.033*
Hypoechoic	−1.960	0.141	0.025–0.789	0.026*
Posterior acoustic features				
Enhancement				0.032*
No posterior acoustic features	1.470	4.351	0.597–31.735	0.147
Shadowing & Combined pattern	1.785	25.924	2.267–296.441	0.009*
BI-RADS category[a]	−1.076	0.341	0.063–1.835	0.210

VTIQ = virtual touch tissue imaging and quantification, OR = odd ratio, CI = confidence interval.

[a] BI-RADS category is divided into two groups :3 ; 4a, 4b, 4c and 5, the reference category was 3.

* Indicates statistically significant difference.

Table 5
Correlation of histologic grade and false negative VTIQ finding of infiltrating carcinomas.

Characteristics	β	OR	95% CI	*P* value
Histologic grade				
1				0.015*
2	2.996	20.000	2.521–158.678	0.005*
3	1.992	7.333	1.372–39.183	0.020*

VTIQ = virtual touch tissue imaging and quantification, OR = odd ratio, CI = confidence interval.

* Indicates statistically significant difference.

Table 6
Independent factors related to false negative VTIQ finding of malignant breast lesions.

Characteristics	β	OR	95% CI	*P* value
Internal calcifications feature	0.623	1.881	0.513–6.904	0.341
BI-RADS category				
3-4a				0.554
4b	−0.147	0.864	0.165–4.524	0.862
4c	0.344	1.411	0.271–7.336	0.683
5	1.264	3.538	0.415–30.148	0.248
Invasive status	1.832	6.193	1.246–30.790	0.026*

VTIQ = virtual touch tissue imaging and quantification, OR = odd ratio, CI = confidence interval.

* Indicates statistically significant difference.

was 9.8% and the FNR was 19.2%. Kapetas et al. [15] reported a higher FPR (17.6%) and FNR (20.6%) than that found in our study, but these investigators used an SWS-max cut-off value of 3.23 m/s. This could be attributable to the divergent SWS measurement protocols and to the larger sample size in our study.

It has been reported that the diameter of breast lesions does not influence elastography results [22], but this was contradictory to our results. We found that the FPR of the most superficial lesions (≤3 mm) was significantly higher (OR: 14.71) than that of the deepest lesions (> 7 mm), which was consistent with Park et al. [23]. The stiffness of larger and more superficial breast lesions was higher than that of the smaller and deeper lesions. This result may be explained by the fact that it is difficult for even an experienced radiologist to perform VTIQ when applying the probe evenly to the skin above larger and more convex lesions without adding compression force. In addition, we found that false-positive VTIQ results were more often found in lesions with shadowing and a combined pattern. Shadowing, as a posterior acoustic feature of a benign breast lesion, may be caused by pathological changes, such as calcifications and focal fibroplasia. Calcifications [24] and focal fibroplasia may also increase the stiffness of the tissue, which can lead to false-positive SWS-max findings.

There were no significant differences in the immunohistochemistry status (ER, PR, HER-2, Ki-67) among false-negative VTIQ findings, which is concordant with previous studies [17,25]. Evans et al. [26] found that the stiffness of a breast lesion, based on SWE, was an independent predictor of axillary lymph node metastasis, which was inconsistent with the results of our study. In contrast, Youk et al. [27] reported that axillary lymph node metastasis was not an independent factor that influenced the stiffness of the breast lesion based on SWE. As opinions vary, further research should be conducted that would focus on the correlation between the stiffness of the breast lesion and axillary lymph node metastasis.

In addition, we analyzed whether the invasive status of all malignant carcinomas and the histologic grade of infiltrating carcinomas might lead to false-negative results. Our results confirmed that non-invasive carcinomas and infiltrating carcinomas with a histologic grade of 1 were more likely to incur false-negative VTIQ results. These results are consistent with the findings of Vinnicombe et al. [17], who indicated that DCIS and low-grade carcinomas were apt to show benign features on 2D-SWE. Considering that assessment of the histological grade of breast cancer relies on the number of mitoses, it is reasonable to postulate that a high-grade cancer with a higher cellularity might show high stiffness on VTIQ [28].

There were several limitations to this study. First, it was a retrospective study in which selection bias might inevitably exist. Second, the sample size of false-positive and false-negative breast lesions on VTIQ was relatively small. Further studies with a larger sample size will need to be undertaken. In addition, some benign lesions were confirmed by CNB and followed in this study, which may have led to false-negative pathological results. Last, there was no analysis of the consistency between intra-observer and inter-observer results in this paper. However, VTIQ is an easy technique to learn and has been shown to have excellent reproducibility [21].

In conclusion, diameter, depth, posterior acoustic features, invasive status, and histologic grade are significant factors in producing false results, while lesions that were larger, more superficial, and which demonstrated shadowing acoustic features on CUS were related to false-positive VTIQ findings. False-negative VTIQ findings were likely to occur in non-invasive carcinomas and in infiltrating carcinomas with a lower histologic category. The findings of this study suggest that these characteristics of breast lesions should be considered when interpreting the results of VTIQ examinations.

Funding

This research did not receive any specific grant from funding agencies in the public, commercial, or not-for-profit sectors.

Conflict of interest

The authors have no conflicts of interest.

References

[1] C. DeSantis, F. Bray, J. Ferlay, J. Lortet-Tieulent, B. Anderson, A. Jemal, International variation in female breast Cancer incidence and mortality rates, Cancer Epidemiol. Biomarkers Prev. 24 (10) (2015) 1495–1506, https://doi.org/10.1158/1055-9965.EPI-15-0535.

[2] T. Kumm, M. Szabunio, Elastography for the characterization of breast lesions: initial clinical experience, Cancer Control 17 (3) (2010) 156–161, https://doi.org/

10.1177/107327481001700303.
[3] S. Srinivasan, T. Krouskop, J Ophir. A quantitative comparison of modulus images obtained using nanoindentation with strain elastograms, Ultrasound Med. Biol. 30 (7) (2004) 899–918, https://doi.org/10.1016/j.ultrasmedbio.2004.05.005.
[4] J. Zhou, W. Zhan, C. Chang, J. Zhang, Z. Yang, Y. Dong, C. Zhou, Y. Song, Role of acoustic shear wave velocity measurement in characterization of breast lesions, J. Ultrasound Med. 32 (2) (2013) 285–294 https://www.ncbi.nlm.nih.gov/pubmed/23341385.
[5] J. Chang, W. Moon, N. Cho, A. Yi, H. Koo, W. Han, D. Noh, H. Moon, S. Kim, Clinical application of shear wave elastography (SWE) in the diagnosis of benign and malignant breast diseases, Breast Cancer Res. Treat. 129 (1) (2011) 89–97, https://doi.org/10.1007/s10549-011-1627-7.
[6] R. Barr, S. Destounis, L. Lackey, W. Svensson, C. Balleyguier, C. Smith, Evaluation of breast lesions using sonographic elasticity imaging: a multicenter trial, J. Ultrasound Med. 31 (2) (2012) 281–287 https://www.ncbi.nlm.nih.gov/pubmed/22298872.
[7] H. Zhi, B. Ou, X. Xiao, Y. Peng, Y. Wang, L. Liu, Y. Xiao, S. Liu, C. Wu, Y. Jiang, S. Parajuly, P. Xu, Y. Hao, J. Li, B. Luo, Ultrasound elastography of breast lesions in chinese women: a multicenter study in China, Clin. Breast Cancer 13 (5) (2013) 392–400, https://doi.org/10.1016/j.clbc.2013.02.015.
[8] G. Li, D. Li, Y. Fang, Y. Song, Z. Deng, J. Gao, Y. Xie, T. Yin, L. Ying, K. Tang, Performance of shear wave elastography for differentiation of benign and malignant solid breast masses, PLoS One 8 (10) (2013) e76322, , https://doi.org/10.1371/journal.pone.0076322.
[9] M. Tozaki, M. Saito, J. Benson, L. Fan, S Isobe. Shear wave velocity measurements for differential diagnosis of solid breast masses: a comparison between virtual touch quantification and virtual touch IQ, Ultrasound Med. Biol. 39 (12) (2013) 2233–2245, https://doi.org/10.1016/j.ultrasmedbio.2013.07.012.
[10] Z. Li, J. Sun, J. Zhang, D. Hu, Q. Wang, K Peng. Quantification of acoustic radiation force impulse in differentiating between malignant and benign breast lesions, Ultrasound Med. Biol. 40 (2) (2014) 287–292, https://doi.org/10.1016/j.ultrasmedbio.2013.09.020.
[11] D. Li, H. Xu, L. Guo, X. Bo, X. Li, R. Wu, J. Xu, Y. Zhang, K. Zhang, Combination of two-dimensional shear wave elastography with ultrasound breast imaging reporting and data system in the diagnosis of breast lesions: a new method to increase the diagnostic performance, Eur. Radiol. 26 (9) (2016) 3290–3300, https://doi.org/10.1007/s00330-015-4163-8.
[12] X. Li, H. Xu, X. Bo, B. Liu, X. Huang, D. Li, L. Guo, J. Xu, L. Sun, L. Fang, X. Xu, Value of virtual touch tissue imaging quantification for evaluation of ultrasound breast imaging-reporting and data system category 4 lesions, Ultrasound Med. Biol. 42 (9) (2016) 2050–2057, https://doi.org/10.1016/j.ultrasmedbio.2016.04.002.
[13] Y. Zhang, C. Zhao, X. Li, Y. He, W. Ren, C. Zou, Y. Du, H. Xu, Virtual touch tissue imaging and quantification: value in malignancy prediction for complex cystic and solid breast lesions, Sci. Rep. 7 (1) (2017) 7807, https://doi.org/10.1038/s41598-017-07865-7.
[14] M. Yao, R. Wu, G. Xu, L. Zhao, H. Liu, H. Pu, Y. Fang, A novel two-dimensional quantitative shear wave elastography to make differential diagnosis of breast lesions: comprehensive evaluation and influencing factors, Clin. Hemorheol. Microcirc. 64 (2) (2016) 223–233, https://doi.org/10.3233/ch-16188.
[15] P. Kapetas, K. Pinker-Domenig, R. Woitek, P. Clauser, M. Bernathova, C. Spick, T. Helbich, P. Baltzer, Clinical application of Acoustic Radiation Force Impulse Imaging with Virtual Touch IQ in breast ultrasound: diagnostic performance and reproducibility of a new technique, Acta Radiol. 58 (2) (2017) 140–147, https://doi.org/10.1177/0284185116641347.
[16] J. Yoon, H. Jung, J. Lee, K. Ko, Shear-wave elastography in the diagnosis of solid breast masses: what leads to false-negative or false-positive results? Eur. Radiol. 23 (9) (2013) 2432–2440, https://doi.org/10.1007/s00330-013-2854-6.
[17] S. Vinnicombe, P. Whelehan, K. Thomson, D. McLean, C. Purdie, L. Jordan, S. Hubbard, A. Evans, What are the characteristics of breast cancers misclassified as benign by quantitative ultrasound shear wave elastography? Eur. Radiol. 24 (4) (2014) 921–926, https://doi.org/10.1007/s00330-013-3079-4.
[18] M. Kim, N. Choi, J. Yang, Y. Yoo, K. Park, False positive or negative results of shear-wave elastography in differentiating benign from malignant breast masses: analysis of clinical and ultrasonographic characteristics, Acta Radiol. 56 (10) (2015) 1155–1162, https://doi.org/10.1177/0284185114551400.
[19] C. S E D'Orsi, E. Mendelson, E. Morris, Breast Imaging Reporting and Data System, 5th ed., American College of Radiology, Reston, VA, 2013.
[20] D. Li, H. Xu, B. Liu, X. Bo, X. Li, R. Wu, Quality measurement of two-dimensional shear wave speed imaging for breast lesions: the associated factors and the impact to diagnostic performance, Sci. Rep. 7 (1) (2017) 5076, https://doi.org/10.1038/s41598-017-05281-5.
[21] M. Golatta, M. Schweitzer-Martin, A. Harcos, S. Schott, C. Gomez, A. Stieber, G. Rauch, C. Domschke, J. Rom, F. Schütz, C. Sohn, J. Heil, Evaluation of virtual touch tissue imaging quantification, a new shear wave velocity imaging method, for breast lesion assessment by ultrasound, Biomed Res. Int. 2014 (2014) 960262, , https://doi.org/10.1155/2014/960262.
[22] G. Sadigh, R.C. Carlos, C.H. Neal, S. Wojcinski, B.A. Dwamena, Impact of breast mass size on accuracy of ultrasound elastography vs. Conventional B-mode ultrasound: a meta-analysis of individual participants, Eur. Radiol. 23 (4) (2013) 1006–1014, https://doi.org/10.1007/s00330-012-2682-0.
[23] S. Park, J. Choi, B. Han, E. Ko, E. Ko, Shear wave elastography in the diagnosis of breast non-mass lesions: factors associated with false negative and false positive results, Eur. Radiol. 27 (9) (2017) 3788–3798, https://doi.org/10.1007/s00330-017-4763-6.
[24] A. Gregory, M. Mehrmohammadi, M. Denis, M. Bayat, D.L. Stan, M. Fatemi, A. Alizad, Effect of calcifications on breast ultrasound shear wave elastography: an investigational study, PLoS One 10 (9) (2015) e0137898, , https://doi.org/10.1371/journal.pone.0147462.
[25] M. Hayashi, Y. Yamamoto, A. Sueta, M. Tomiguchi, M. Yamamoto-Ibusuki, T. Kawasoe, A. Hamada, H. Iwase, Associations between elastography findings and clinicopathological factors in breast Cancer, Medicine (Baltimore) 94 (50) (2015) e2290, , https://doi.org/10.1097/MD.0000000000002290.
[26] A. Evans, P. Rauchhaus, P. Whelehan, K. Thomson, C. Purdie, L. Jordan, C. Michie, A. Thompson, S. Vinnicombe, Does shear wave ultrasound independently predict axillary lymph node metastasis in women with invasive breast cancer? Breast Cancer Res. Treat. 143 (1) (2014) 153–157, https://doi.org/10.1007/s10549-013-2747-z.
[27] J. Youk, H. Gweon, E. Son, J. Kim, J. Jeong, Shear-wave elastography of invasive breast cancer: correlation between quantitative mean elasticity value and immunohistochemical profile, Breast Cancer Res. Treat. 138 (1) (2013) 119–126, https://doi.org/10.1007/s10549-013-2407-3.
[28] L. Martincich, V. Deantoni, I. Bertotto, S. Redana, F. Kubatzki, I. Sarotto, V. Rossi, M. Liotti, R. Ponzone, M. Aglietta, D. Regge, F. Montemurro, Correlations between diffusion-weighted imaging and breast cancer biomarkers, Eur. Radiol. 22 (7) (2012) 1519–1528, https://doi.org/10.1007/s00330-012-2403-8.